

Beta Canis Majoris: The Other Major Ionization Source of the Local Interstellar Clouds

J. MICHAEL SHULL,^{1,2} RACHEL M. CURRAN,³ AND MICHAEL W. TOPPING⁴

¹*Department of Astrophysical & Planetary Sciences, University of Colorado, Boulder, CO 80309, USA; michael.shull@colorado.edu*

²*Department of Physics and Astronomy, University of North Carolina, Chapel Hill, NC 27599, USA;*

³*Department of Physics & Astronomy, University of North Carolina, Chapel Hill, NC 27599 USA;*

⁴*Steward Observatory, University of Arizona, Tucson, AZ 85721, USA*

ABSTRACT

Two nearby B-type stars, ϵ CMa (124 ± 2 pc) and β CMa (151 ± 5 pc), are important contributors to the photoionization of the local interstellar cloud (LIC). At spectral type B1 II-III, β CMa is slightly hotter than ϵ CMa (B2 II-III), but its ionizing flux at Earth is attenuated by a much larger H I column density. At the external surface of the LIC, the two stars produce similar fluxes in the Lyman continuum (LyC). From the β CMa angular diameter, bolometric flux, and position on the Hertzsprung-Russell diagram, we obtain a consistent set of stellar parameters: $T_{\text{eff}} = 25,180 \pm 1120$ K, $\log g = 3.70 \pm 0.08$, radius $R = 8.44 \pm 0.56 R_{\odot}$, mass $M = 13 \pm 1 M_{\odot}$, and luminosity $L = 10^{4.41 \pm 0.06} L_{\odot}$. The EUVE-observed fluxes and non-LTE model atmospheres are used to determine the ionizing photon production rate $Q_{\text{H}} = 10^{46.0 \pm 0.1} \text{ s}^{-1}$ and fluxes incident on the local clouds, $\Phi_{\text{HI}} \approx 3700 \text{ cm}^{-2} \text{ s}^{-1}$ and $\Phi_{\text{HeI}} \approx 110 \text{ cm}^{-2} \text{ s}^{-1}$ in the H I and He I continua. The corresponding photoionization rates are $\Gamma_{\text{HI}} \approx 1.5 \times 10^{-14} \text{ s}^{-1}$ and $\Gamma_{\text{HeI}} \approx 7.3 \times 10^{-16} \text{ s}^{-1}$. Within the local cloud, the LyC flux is attenuated by an H I column density $N_{\text{HI}} = (1.9 \pm 0.1) \times 10^{18} \text{ cm}^{-2}$, with optical depth $\tau_{\text{LL}} = 12.0 \pm 0.6$ at the Lyman limit. The radial velocities and proper motions of β CMa and ϵ CMa indicate that both stars passed within 10 ± 1 pc of the Sun approximately 4.4 Myr ago, with incident ionizing fluxes 180–200 times larger. Their EUV radiation photoionized and heated the tunnel in the local interstellar gas, associated dynamically with past supernova explosions in the Sco-Cen OB association.

1. INTRODUCTION

The B-type giant star Beta Canis Majoris (β CMa), also known as HD 44743 and Mirzam, is one of several bright sources of extreme ultraviolet (EUV) radiation (J. Dupuis et al. 1995; J. Vallergera & B. Welsh 1995; N. Craig et al. 1997) observed by the Extreme Ultraviolet Explorer (EUVE). Both ϵ CMa and β CMa are located in the direction ($\ell = 232 \pm 5$, $b = -15 \pm 4$) of a low-density, highly ionized tunnel in the interstellar medium (P. Frisch & D. York 1983; C. Gry et al. 1985; B. Welsh 1991; J. Vallergera 1998; D. Sfeir et al. 1999; J. Linsky et al. 2019). Both stars contribute to the H I photoionization rate of the Local Interstellar Cloud or LIC (J. Vallergera 1998). A portion of the β CMa ionizing spectrum was measured by EUVE between 504–720 Å. However, any flux between 750–912 Å would have been highly attenuated by the interstellar medium (ISM). After correcting for ISM absorption, we find that β CMa and ϵ CMa have comparable fluxes in the Lyman continuum (LyC) incident on the surface of the local clouds.

In our previous paper (J. M. Shull et al. 2025) we analyzed the stellar parameters of ϵ CMa, and derived the intervening H I column density and the H I photoionization rate. In this paper, we provide similar calculations of the stellar parameters of β CMa, the ISM column density, and photoionization rates of H I and He I. We employ non-LTE, line-blanketed model atmospheres to anchor the relative fluxes in the stellar EUV continuum shortward of the ionization edges of H I ($\lambda \leq 911.75$ Å) and He I ($\lambda \leq 504.26$ Å). We then use observed fluxes in the EUV (504–720 Å) and far-UV (1000–1400 Å) to determine the attenuation of the LyC radiation in both the stellar atmosphere and ISM.

In Section 2, we derive a consistent set of stellar parameters (radius, mass, effective temperature, luminosity) based on measurements of the parallax distance, stellar angular diameter, and total flux. In Section 3, we analyze the EUV flux attenuation in the stellar atmosphere and derive an interstellar H I column density, $N_{\text{HI}} = (1.9 \pm 0.1) \times 10^{18} \text{ cm}^{-2}$, corresponding to an H I optical depth $\tau_{\text{LL}} = 12.0 \pm 0.6$ at the Lyman limit (LL). The non-LTE stellar model atmosphere

predicts a flux decrement factor of $\Delta_{\text{LL}} = 67 \pm 7$ at 912 Å but shows little absorption at the He I ionization edge (504 Å). This is evidently a non-LTE effect of backwarming from the line-blanketed B-star wind. In Section 4 we discuss the implications of our results for the ionization structure of the local interstellar clouds. We find that ϵ CMa and β CMa have comparable photoionization rates of H I at the external surface of the local clouds. However, β CMa has a much larger ionization rate of He I, owing to its higher effective temperature $T_{\text{eff}} \approx 25,000$ K, compared to 21,000 K for ϵ CMa.

2. REVISED PROPERTIES OF BETA CANIS MAJORIS

2.1. Basic Stellar Parameters

In a classic survey of southern B-type stars, J. Lesh (1968) listed the spectral type (SpT) of β CMa as B1 II-III, with apparent and absolute visual magnitudes ($m_V = 1.97$, $M_V = -4.57$) and a spectrophotometric distance of 203 pc. A SpT of B1 II-III was confirmed by I. Negueruela et al. (2024). However, the *Hipparcos* parallax measurement of 6.62 ± 0.22 mas (F. van Leeuwen 2007) provided a shorter distance $d = 151 \pm 5$ pc, with a modulus ($m_V - M_V$) = 5.895 ± 0.071 smaller by 0.64 mag. In other papers, the distance to β CMa was quoted variously as 213 pc (R. Bohlin 1975), 206 pc (B. Savage et al. 1977; R. Bohlin et al. 1978; J. Cassinelli et al. 1996), and 203 pc (B. Welsh 1991; J. M. Shull & M. Van Steenberg 1985). The new distance modulus implies an absolute magnitude $M_V = -3.925 \pm 0.071$, similar to the value of -4.0 given in J. Lesh (1968) for B1 III spectral type.

A key physical measurement for β CMa is its angular diameter $\theta_d = 0.52 \pm 0.03$ mas (R. Hanbury Brown et al. 1974) found with the stellar interferometer at the Narrabri Observatory. From this and a parallax distance $d = 151 \pm 5$ pc, we derive a stellar radius of

$$R = \left(\frac{\theta_d d}{2} \right) = 5.87 \times 10^{11} \text{ cm } (8.44 \pm 0.56 R_{\odot}), \quad (1)$$

where we combined the relative errors on θ_d (5.8%) and d (3.3%) in quadrature. The revision in the β CMa distance from 203 pc to 151 pc also changes its inferred mass and surface gravity. L. Fossati et al. (2015) used the new distance $d = 151 \pm 5$ pc and evaluated the radius and mass from two sets of evolutionary models: $R = 7.4^{+0.8}_{-0.9} R_{\odot}$ and $M = 12.0^{+0.3}_{-0.7} M_{\odot}$ (tracks from C. Georgy et al. 2013) and $R = 8.2^{+0.6}_{-0.5} R_{\odot}$ and $M = 12.6^{+0.4}_{-0.5} M_{\odot}$ (tracks from L. Brott et al. 2011). These radii are in good agreement with our radius ($8.44 \pm 0.56 R_{\odot}$) and the $13 \pm 1 M_{\odot}$ gravitational and evolutionary masses that we derive below.

The absolute magnitude and bolometric magnitude of β CMa need revision based on its new distance $d = 151 \pm 5$ pc, but the stellar classification has remained consistent at B1 II-III (J. Lesh 1968; L. Fossati et al. 2015; I. Negueruela et al. 2024). At this SpT, the absolute magnitude $M_V = -4.0$ (J. Lesh 1968 value at B1.5 III), and we adopt a bolometric correction ($M_{\text{bol}} - M_V$) ≈ -2.5 from Figure 5 of M. Pedersen et al. (2020) at $T_{\text{eff}} = 25,000$ K and $\log g = 3.5$ – 4.0 . This yields a bolometric absolute magnitude $M_{\text{bol}} = -6.425 \pm 0.07$ and luminosity of $10^{4.47} L_{\odot}$, based on the solar bolometric absolute magnitude $M_{\text{bol},\odot} = 4.74$. This luminosity comes with some uncertainty from the applied bolometric correction.

Values of R , T_{eff} , g , and L must satisfy the relations $g = (GM/R^2)$ and $L = 4\pi R^2 \sigma_{\text{SB}} T_{\text{eff}}^4$, where $\sigma_{\text{SB}} = 5.6705 \times 10^{-5} \text{ erg cm}^{-2} \text{ s}^{-1} \text{ K}^{-4}$ is the Stefan-Boltzmann constant and $R = (\theta_d d/2)$. Here, $\theta_d = 2.52 \times 10^{-9} \text{ rad}$ (0.52 ± 0.03 mas) is the measured stellar angular diameter (R. Hanbury Brown et al. 1974). The integrated stellar flux is $f = (36.2 \pm 4.9) \times 10^{-6} \text{ erg cm}^{-2} \text{ s}^{-1}$ from A. Code et al. (1976), who combined ground-based visual and near-infrared photometry with ultraviolet observations (1100–3500 Å) taken by the Orbiting Astronomical Observatory (OAO-2). This flux included an extrapolated value for shorter wavelengths $f(\lambda \leq 1100 \text{ Å}) = (7.5 \pm 3.8) \times 10^{-6} \text{ erg cm}^{-2} \text{ s}^{-1}$. Even after correcting the observed EUV flux for interstellar absorption, the Lyman continuum represents less than 1% of the bolometric flux. The constraints from stellar angular diameter and total flux give a useful relation for the bolometric effective temperature $T_{\text{eff}} = (4f/\sigma_{\text{SB}} \theta_d^2)^{1/4}$,

$$T_{\text{eff}} = (25,180 \pm 1120 \text{ K}) \left(\frac{f}{36.2 \times 10^{-6}} \right)^{1/4} \left(\frac{\theta_d}{0.52 \text{ mas}} \right)^{-1/2}. \quad (2)$$

The stellar radius and bolometric relation with T_{eff} suggest a total luminosity,

$$L \approx (25,800 \pm 3900 L_{\odot}) \left(\frac{T_{\text{eff}}}{25,180 \text{ K}} \right)^4 \left(\frac{R}{8.44 R_{\odot}} \right)^2. \quad (3)$$

With the relative errors on parallax distance (3.3%) and integrated flux (13.5%), this luminosity estimate, $L = 10^{4.41 \pm 0.06} L_{\odot}$, has a 15% uncertainty, and it is also 15% lower than our estimate $L = 10^{4.47 \pm 0.07}$ from photometry and bolometric correction. Both luminosities agree within their propagated uncertainties using the relations $L = 4\pi d^2 f = 4\pi R^2 \sigma_{\text{SB}} T_{\text{eff}}^4$. Our values, $T_{\text{eff}} = 25,180 \text{ K}$ and $L = 10^{4.41 \pm 0.06}$, are similar to the luminosity quoted in L. Fossati et al. (2015). **Table 1** summarizes the stellar parameters from this work and previous papers.

2.2. Stellar Atmospheres and EUV Fluxes

For β CMa, J. Cassinelli et al. (1996) discussed two sets of stellar atmosphere parameters (T_{eff} and $\log g$). Following the method of A. Code et al. (1996), they used the observed total flux and angular diameter to find $T_{\text{eff}} = 25,180 \text{ K}$, the same as ours (eq. [2]) using the same method. However, their value of surface gravity ($\log g = 3.4$) is lower than our value of 3.7. They also discussed possible lower temperatures, $T_{\text{eff}} = 23,250 \text{ K}$, with $\log g = 3.5$, that were in better agreement with their line-blanketed model atmospheres. However, they also noted that the higher T_{eff} models gave better agreement with the observed EUV fluxes⁵. At their larger adopted distance, $d = 206 \text{ pc}$, the implied stellar parameters ($R \approx 11.5 R_{\odot}$ and $M = gR^2/G \approx 24 M_{\odot}$) are discrepant with the derived position of β CMa on the H-R diagram. In a spectroscopic analysis of β CMa, L. Fossati et al. (2015) found $T_{\text{eff}} = 24,700 \pm 300 \text{ K}$ and $\log g = 3.78 \pm 0.08$.

For consistency with the key observed parameters (distance, total flux, interferometric diameter), we adopt $T_{\text{eff}} = 25,180 \pm 1120 \text{ K}$ and $\log g = 3.70 \pm 0.08$ ($g = GM/R^2 = 5010 \pm 500 \text{ cm s}^{-2}$). With a measured rotational velocity $V_{\text{rot}} \sin i = 20.3 \pm 7.2 \text{ km s}^{-1}$ (L. Fossati et al. 2015), we can neglect the centrifugal term, $V_{\text{rot}}^2/R \approx (7 \text{ cm s}^{-2})(\sin i)^{-2}$ and infer a gravitational mass ($M = gR^2/G$) of

$$M = (13 \pm 3 M_{\odot}) \left(\frac{g}{5010 \text{ cm s}^{-2}} \right) \left(\frac{R}{8.44 R_{\odot}} \right)^2. \quad (4)$$

The quoted error on M includes uncertainties in surface gravity and radius, added in quadrature with $(\sigma_M/M)^2 = (\sigma_g/g)^2 + (2\sigma_R/R)^2$. This gravitational mass is consistent with its evolutionary mass on the H-R diagram, $M_{\text{evol}} = 13 \pm 1 M_{\odot}$. **Figure 1** shows this location at $\log(L/L_{\odot}) = 4.41$ and $T_{\text{eff}} = 25,180 \text{ K}$, with evolutionary tracks from L. Brott et al. (2011). This position is consistent with luminosity class II/III (giant), and it places β CMa within the β Cephei instability strip, consistent with its observed pulsations. This conclusion is confirmed by comparison with the locus of radial and non-radial instability modes in Figs. 2 and 3 of L. Deng & D. R. Xiong (2001).

3. INTERSTELLAR ABSORPTION AND H I COLUMN DENSITY

3.1. Previous Column Density Estimates

The EUVE observations of β CMa (J. Cassinelli et al. 1996; Craig et al. 1997) showed detectable flux between 510 Å and 720 Å, but no flux was detected below the He I edge ($\lambda \leq 504.26 \text{ Å}$) or He II edge ($\lambda < 227.84 \text{ Å}$). The lack of observed He I continuum flux is almost certainly the result of the large optical depth ($\tau \approx 3.35$ at 504 Å) arising from H I and He I photoelectric absorption in the intervening ISM. The two B-type stars, ϵ CMa and β CMa, are the strongest sources of EUV radiation as viewed from low-Earth orbit (J. Vallergera & B. Welsh 1995). This is primarily a result of their location in a low-density cavity or “interstellar tunnel” (C. Gry et al. 1985; B. Welsh 1991; J. Vallergera

⁵ Cassinelli et al. (1996) suggested that backwarming by the shocked stellar wind could boost the temperature in the upper atmosphere where the Lyman continuum is formed. A similar non-LTE wind effect was proposed by F. Najarro et al. (1996), involving doppler shifts and velocity-induced changes in density that affect the escape of H I and He I resonance lines and their ground-state populations. Both mechanisms are sensitive to mass-loss rates in the range $\dot{M} \approx (1-10) \times 10^{-9} M_{\odot} \text{ yr}^{-1}$.

et al. 1998). In order to find the photoionizing flux incident on the exterior surface of the local clouds, we must correct for EUV flux attenuation by H I and He I.

Previous estimates of the amount of interstellar hydrogen toward β Cma were somewhat uncertain. The *Copernicus* spectroscopic fits to the wings of the interstellar Ly α absorption line set upper limits of $N_{\text{HI}} < 5 \times 10^{18} \text{ cm}^{-2}$ (R. Bohlin 1975; R. Bohlin et al. 1978) and $N_{\text{HI}} < 3 \times 10^{18} \text{ cm}^{-2}$ (J. M. Shull & M. Van Steenberg 1985). The latter limit corresponds to an optical depth $\tau_{\text{LL}} < 19$ at 912 Å. The actual ISM column density is less, since some EUV flux penetrates the local clouds. The EUVE fluxes (510–720 Å) detected by EUVE (J. Cassinelli et al. 1996) were combined with stellar atmosphere models to estimate an interstellar column density $N_{\text{HI}} = (2.0\text{--}2.2) \times 10^{18} \text{ cm}^{-2}$. In the next subsection, we make similar calculations and find a lower value, $N_{\text{HI}} = (1.9 \pm 0.1) \times 10^{18} \text{ cm}^{-2}$.

3.2. Photoelectric Absorption

In our previous study of ϵ Cma (J. M. Shull et al. 2025) we derived the intervening H I column density by comparing the observed EUV and FUV continuum fluxes from 300–1150 Å to non-LTE model atmospheres. By exploring various attenuation models, we found an interstellar column density $N_{\text{HI}} = (6 \pm 1) \times 10^{17} \text{ cm}^{-2}$. For β Cma, with less complete coverage of the EUV, we modified the method to compare EUVE and model fluxes at four wavelengths (700, 650, 600, 570 Å) and anchored to the observed fluxes at 1000–1200 Å from Voyager and International Ultraviolet Explorer (IUE).

The expected FUV/EUV continua were based on model atmospheres produced with the code **WM-basic** developed by A. Pauldrach et al. (2001)⁶. We chose this code because of its hydrodynamic solution of expanding atmospheres with line blanketing and non-LTE radiative transfer, including its treatment of the continuum and wind-blanketing from EUV lines. Extensive discussion of hot-star atmosphere codes appears in papers by D. J. Hillier & D. Miller (1998), F. Martins et al. (2005), and C. Leitherer et al. (2014). We restore the observed continuum to its shape at the stellar surface by multiplying the observed flux by $\exp(\tau_{\lambda})$, using optical depths τ_{λ} of photoelectric absorption in the ionizing continua of H I ($\lambda \leq 912$ Å) and He I ($\lambda \leq 504$ Å),

$$\tau_{\text{HI}}(\lambda) \approx (6.304) \left(\frac{N_{\text{HI}}}{10^{18} \text{ cm}^{-2}} \right) \left(\frac{\lambda}{912 \text{ Å}} \right)^3, \quad (5)$$

$$\tau_{\text{HeI}}(\lambda) \approx (0.737) \left(\frac{N_{\text{HeI}}}{10^{17} \text{ cm}^{-2}} \right) \left(\frac{\lambda}{504 \text{ Å}} \right)^{1.63}. \quad (6)$$

These approximations are based on power-law fits to the photoionization cross sections at wavelengths below threshold, $\sigma_{\text{HI}}(\lambda) \approx (6.304 \times 10^{-18} \text{ cm}^2)(\lambda/912 \text{ Å})^3$ (D. Osterbrock & G. Ferland 2006) and $\sigma_{\text{HeI}}(\lambda) \approx (7.37 \times 10^{-18} \text{ cm}^2)(\lambda/504 \text{ Å})^{1.63}$ (D. Samson et al. 1994). In our actual calculations, we used the exact (non-relativistic) H I cross section (Bethe & Salpeter 1957),

$$\sigma_{\nu} = \sigma_0 \left(\frac{\nu}{\nu_0} \right)^{-4} \frac{\exp[4 - (4 \arctan \epsilon)/\epsilon]}{[1 - \exp(-2\pi/\epsilon)]}. \quad (7)$$

Here, the dimensionless parameter $\epsilon \equiv [(\nu/\nu_0) - 1]^{1/2}$ with frequency ν_0 defined at the ionization energy $h\nu_0 = 13.598 \text{ eV}$ and $\sigma_0 = 6.304 \times 10^{-18} \text{ cm}^2$. The two formulae agree at threshold $\nu = \nu_0$, but the approximate formula deviates increasingly at shorter wavelengths. The exact cross section is higher by 8.2% (700 Å), 12.3% (600 Å), and 16.4% (500 Å).

In the far-UV, the stellar continuum in the non-LTE model atmosphere rises slowly from 1150 Å down to 1000 Å, and then declines owing to absorption in higher Lyman-series lines converging on the LL at 911.75 Å. For reference, a pure blackbody at $T = 25,180 \text{ K}$ peaks at $\lambda_{\text{max}} \approx 1160 \text{ Å}$. However, there is still some uncertainty in the spectral shape from 1150 Å down to 912 Å, a region unobserved by IUE. The Voyager observations, plotted in Figure 2a of J. Cassinelli et al. (1996), show a peak in $F_{\lambda} \approx 4 \times 10^{-8} \text{ erg cm}^{-2} \text{ s}^{-1} \text{ Å}^{-1}$ around 1000 Å, similar to the mean flux seen in IUE (SWP Large Aperture) archival spectra at 1150 Å.

⁶ This code can be found at <http://www.usm.uni-muenchen.de/people/adi/Programs/Programs.html>

For our flux attenuation calculations, we adopt a continuum level at 912^+ \AA , just longward of the Lyman edge, of $F_\lambda = 4 \times 10^{-8} \text{ erg cm}^{-2} \text{ s}^{-1} \text{ \AA}^{-1}$. This corresponds to a photon flux of $\Phi(912^+) = 1836 \text{ photons cm}^{-2} \text{ s}^{-1} \text{ \AA}^{-1}$. In the **WM-basic** model atmosphere (**Figure 2**), the stellar flux drops by a factor $F(912^+)/F(912^-) = 67 \pm 7$. We then compare the model fluxes to the photon fluxes $\Phi(\lambda) = \lambda F_\lambda / hc$ at four EUVE-observed wavelengths, with photon fluxes ($\text{photons cm}^{-2} \text{ s}^{-1} \text{ \AA}^{-1}$) of 0.02 (700 \AA), 0.05 (650 \AA), 0.085 (600 \AA), and 0.11 (570 \AA). After converting F_λ to Φ_λ , we predict model photon flux ratios of

$$\Delta(700) = \Phi(912^+)/\Phi(700) = 209 \quad (8)$$

$$\Delta(650) = \Phi(912^+)/\Phi(650) = 468 \quad (9)$$

$$\Delta(600) = \Phi(912^+)/\Phi(600) = 788 \quad (10)$$

$$\Delta(570) = \Phi(912^+)/\Phi(570) = 1179. \quad (11)$$

Combining the observed photon fluxes, model flux ratios, and anchor flux $\Phi(912^+)$, we arrive at estimates of the ISM optical depth,

$$\tau_{\text{ISM}} = \ln \left[\frac{\Phi(912^+)/\Phi(\lambda)}{\Delta(\lambda)} \right], \quad (12)$$

with a corresponding H I column density $N_{\text{HI}} = \tau_{\text{ISM}}/\sigma_{\text{HI}}(\lambda)$. The most reliable estimates come from data and models at 700 \AA ($\sigma_{\text{HI}} = 3.086 \times 10^{-18} \text{ cm}^2$) and 650 \AA ($\sigma_{\text{HI}} = 2.516 \times 10^{-18} \text{ cm}^2$), for which we obtain:

$$\tau_{\text{ISM}}(700 \text{ \AA}) = 5.964 \text{ and } N_{\text{HI}} = 1.93 \times 10^{18} \text{ cm}^{-2} \quad (13)$$

$$\tau_{\text{ISM}}(650 \text{ \AA}) = 4.608 \text{ and } N_{\text{HI}} = 1.83 \times 10^{18} \text{ cm}^{-2}. \quad (14)$$

We adopt a mean value $N_{\text{HI}} = (1.9 \pm 0.1) \times 10^{18} \text{ cm}^{-2}$, with optical depth $\tau_{\text{ISM}} = 12.0 \pm 0.6$ at the Lyman limit. The stellar atmosphere produces a LL flux decrement factor $\Delta_{\text{star}} \approx 67 \pm 7$, and the ISM produces $\Delta_{\text{ISM}} \approx e^{12} \approx 1.6 \times 10^5$. With this much attenuation, there would be little detectable flux from 750 \AA to 912 \AA . The EUVE spectrometers did not observe at wavelengths longward of 730 \AA , and the Colorado Dual-Channel Extreme Ultraviolet Continuum Experiment (DEUCE) spectrograph saw no flux below 912 \AA in its (2 November 2020) rocket flight (Emily Witt, private communication).

3.3. Photoionization Rates Outside the Local Clouds

With our derived interstellar column density toward β Cma of $N_{\text{HI}} = (1.9 \pm 0.1) \times 10^{18} \text{ cm}^{-2}$, we adopt a He I column density $N_{\text{HeI}} = (1.3 \pm 0.2) \times 10^{17} \text{ cm}^{-2}$, based on observations of interstellar ratios of He I/H I toward nearby white dwarfs⁷. The photoionization rates of H I and He I are found by integrating the ionizing photon flux $\Phi_\lambda = (\lambda F_\lambda / hc)$ multiplied by the photoionization cross section σ_λ and the attenuation factor $\exp(-\tau_\lambda)$. For H I ionization, we use the detected EUVE fluxes (504–730 \AA) and an extrapolation of the product $\Phi_\lambda \sigma_\lambda \exp(-\tau_\lambda)$ from 730 \AA to 912 \AA . After correcting for ISM attenuation, we integrate over the ionizing spectrum to find a total photon flux of $\Phi_{\text{H}} = 3700 \pm 1000 \text{ cm}^{-2} \text{ s}^{-1}$ and an H I photoionization rate $\Gamma_{\text{HI}} = 1.5 \times 10^{-14} \text{ s}^{-1}$ at the external surface of the local cloud. These values are comparable to those of ϵ Cma (Shull et al. 2025), with $\Phi_{\text{H}} = 3100 \pm 1000 \text{ cm}^{-2} \text{ s}^{-1}$ and $\Gamma_{\text{HI}} = 1.3 \times 10^{-14} \text{ s}^{-1}$.

For the He I continuum, we again use the non-LTE model atmosphere (**Figure 2**) to establish the flux ratio between the two ionization edges, $F(912^+)/F(504^+) \approx 7000$. The flux falls off rapidly below the He I threshold and is well fitted (between $400 \text{ \AA} \leq \lambda \leq 504 \text{ \AA}$) by the relation $F_\lambda = F_0(\lambda/\lambda_0)^{10}$, with $F_0 = 5.7 \times 10^{-12} \text{ erg cm}^{-2} \text{ s}^{-1} \text{ \AA}^{-1}$ at $\lambda_0 = 504.26 \text{ \AA}$. The He I cross section is $\sigma_{\text{HeI}} \approx \sigma_0(\lambda/\lambda_0)^{1.63}$, where $\sigma_0 = 7.37 \times 10^{-18} \text{ cm}^2$ at 504.26 \AA . We integrate over wavelengths $\lambda \leq \lambda_0$, defining a dimensionless variable $u = (\lambda/\lambda_0)$ and expressing the surface photoionization integral as

$$\Gamma_{\text{HeI}} = \int_0^{\lambda_0} \left[\frac{\lambda F_\lambda}{hc} \right] \sigma_{\text{HeI}}(\lambda) e^{-\tau(\lambda)} d\lambda = \left[\frac{F_0 \sigma_0 \lambda_0^2}{hc} \right] \int_0^1 u^{12.63} e^{-\tau(u)} du. \quad (15)$$

⁷ J. Dupuis et al. (1995) reported a mean ratio $\beta = N_{\text{HI}}/N_{\text{HeI}} \approx 14$, after correcting the observed H I and He I column densities for stellar contributions using LTE, hydrostatic, plane-parallel model atmospheres. The EUVE column densities indicated β ranging from 12.1 ± 3.6 to 18.4 ± 1.3 . Removing the two extreme values, we obtain a mean and rms dispersion of $\beta = 14.5 \pm 1.1$. These values are consistent with earlier sounding-rocket results (J. Green et al. 1990) with $11.5 < \beta < 24$ (90% confidence level) toward the white dwarf G191-B2B.

Similarly, the total flux in the He I ionizing continuum can be expressed as,

$$\Phi_{\text{HeI}} = \int_0^{\lambda_0} \left[\frac{\lambda F_\lambda}{hc} \right] e^{\tau(\lambda)} d\lambda = \left[\frac{F_0 \lambda_0^2}{hc} \right] \int_0^1 u^{11} e^{\tau(u)} du. \quad (16)$$

The two dimensionless integrals are 1.35 (eq. [15]) and 1.46 (eq. [16]), showing increases by factors of 18 (mean $\tau = 2.86$) over the unattenuated integrals (setting $e^\tau = 1$). We then obtain $\Gamma_{\text{HeI}} = 7.3 \times 10^{-16} \text{ s}^{-1}$ and $\Phi_{\text{HeI}} = 107$ photons $\text{cm}^{-2} \text{ s}^{-1}$. Because of its hotter effective temperature, β CMa is an important source of He-ionizing photons in the local cloud, much larger than ϵ CMa for which we estimate $\Gamma_{\text{HeI}} = 4.4 \times 10^{-17} \text{ s}^{-1}$. As noted by J. Dupuis et al. (1995) and J. Vallergera (1998), other sources of He I ionization include three nearby white dwarfs (G191-B2B, Feige 24, HZ 43A).

The hydrogen and helium ionization fractions at the outer surface of the local cloud depend on the ionizing fluxes from two B-type stars (ϵ CMa and β CMa), three white dwarfs, and EUV emission lines produced by hot plasma in the local hot bubble (LHB). The two B-type stars produce a combined LyC photon flux (at the external cloud surface) of $\Phi_{\text{HI}} \approx 6800 \pm 1400 \text{ cm}^{-2} \text{ s}^{-1}$ and hydrogen ionization rate $\Gamma_{\text{HI}} \approx 3 \times 10^{-14} \text{ s}^{-1}$. In photoionization equilibrium, the hydrogen ionization fraction, $x = n_{\text{HII}}/n_{\text{H}}$, is $x = (1/2)[-a + (a^2 + 4a)^{1/2}]$, the solution of $x^2/(1-x) = a$, where the constant $a = [\Gamma_{\text{HI}}/1.1n_{\text{H}}\alpha_{\text{H}}]$. We adopt a hydrogen case-B radiative recombination coefficient (Draine 2011) $\alpha_{\text{H}} = 3.39 \times 10^{-13} \text{ cm}^3 \text{ s}^{-1}$ at $T = 7000 \text{ K}$. The cloud is assumed to have constant hydrogen density $n_{\text{H}} \equiv n_{\text{HI}} + n_{\text{HII}} \approx 0.2 \text{ cm}^{-3}$, and the factor 1.1 accounts for electrons potentially contributed by He^+ . We find $a = 0.402$ and $x = 0.464$ at the surface of the local clouds. If we include the He-ionizing continuum, with $\Gamma_{\text{HeI}} = 7.3 \times 10^{-16} \text{ s}^{-1}$ and solve coupled equations for the H and He ionization equilibrium, we find $x \approx 0.479$ (H^+) and $y \approx 0.022$ (He^+). These ionization fractions decrease with depth into the cloud, as the LyC flux is attenuated.

3.4. Stellar motion and Non-equilibrium Ionization

For β CMa, Hipparcos measurements (F. van Leeuwen 2007) find a parallax distance $d = 151 \pm 5 \text{ pc}$, radial velocity $V_r = 33.7 \pm 0.5 \text{ km s}^{-1}$, and transverse velocity $V_\perp = 2.38 \pm 0.21 \text{ km s}^{-1}$. The transverse velocity is based on its total proper motion $\mu_\perp = -3.32 \pm 0.28 \text{ mas yr}^{-1}$ with components $\mu_\alpha \cos \delta = -3.23 \pm 0.19 \text{ mas yr}^{-1}$ and $\mu_\delta = -0.78 \pm 0.20 \text{ mas yr}^{-1}$ (in RA and Decl). Thus, β CMa passed close to the Sun at a time $t_{\text{pass}} = d/V_r = 4.38 \pm 0.16 \text{ Myr}$ ago, at an offset distance of $d_\perp = \mu_\perp d^2/V_r = 10.6 \pm 1.1 \text{ pc}$. These values are similar to those for ϵ CMa, which passed by the Sun $4.44 \pm 0.10 \text{ Myr}$ at offset distance $9.3 \pm 0.5 \text{ pc}$ (Shull et al. 2025). The ionizing radiation field from these stars would have been 200 times higher than the current value. With the Sun's trajectory moving out of the local cloud, the location of ϵ CMa and β CMa relative to the local hydrogen gas remains uncertain. The local clouds are not self-gravitating and probably gravitationally unbound from the Sun. They may not have been exposed to the same enhanced ionizing radiation field.

Nevertheless, ϵ CMa and β CMa would have produced strong ionizing effects in the past on any nearby interstellar gas. The stellar radial velocities correspond to distance changes of 27.3 pc/Myr (ϵ CMa) and 33.7 pc/Myr (β CMa) away from the Sun. Tracking the enhancements in $\Gamma_{\text{H}}(t)$ along the past trajectories of these stars, we estimate that the hydrogen ionization fraction peaked at $x \approx 0.99$ at closest passage (4.4 Myr ago) and the LIC would have been fully ionized. At 1.6 Myr in the past, when the stars were at distances of 79 pc (ϵ CMa) and 96 pc (β CMa), the equilibrium ionization fraction decreased to $x \approx 0.62$. More recently, the fraction declined to values $x \approx 0.5$. Over the last 1.6 Myr, non-equilibrium ionization effects set in, as the recombination time becomes longer than the photoionization time.

To illustrate this effect, we estimate the time scales for hydrogen photoionization and recombination, and for radiative cooling of gas near the local cloud surface:

$$t_{\text{ph}} = \Gamma_{\text{H}}^{-1} \approx (1 \text{ Myr}) \left(\frac{\Gamma_{\text{H}}}{3 \times 10^{-14} \text{ s}^{-1}} \right)^{-1} \quad (17)$$

$$t_{\text{rec}} = (n_e \alpha_{\text{H}})^{-1} \approx (0.93 \text{ Myr}) \left(\frac{n_e}{0.1 \text{ cm}^{-3}} \right)^{-1} T_{7000}^{0.809} \quad (18)$$

$$t_{\text{cool}} = \frac{3n_{\text{tot}}kT/2}{n_{\text{H}}^2 \Lambda(T)} \approx (11 \text{ Myr}) \left(\frac{n_{\text{H}}}{0.2 \text{ cm}^{-3}} \right)^{-1} T_{7000}. \quad (19)$$

Here, we scaled Γ_{H} to the combined rates for β and ϵ CMa at the LIC and used a case-B radiative recombination rate coefficient $\alpha_{\text{H}} = (3.39 \times 10^{-13} \text{ cm}^3 \text{ s}^{-1}) T_{7000}^{-0.809}$ (B. Draine 2011), appropriate for $T = (7000 \text{ K}) T_{7000}$. We adopted total hydrogen density $n_{\text{H}} \approx 0.2 \text{ cm}^{-3}$, electron density $n_e \approx 0.1 \text{ cm}^{-3}$, and a radiative cooling rate $n_{\text{H}}^2 \Lambda(T)$ with coefficient $\Lambda(T) \approx 3 \times 10^{-26} \text{ erg cm}^3 \text{ s}^{-1}$.

The current timescales for photoionization and recombination are comparable ($\sim 1 \text{ Myr}$), but the radiative cooling time and stellar passing time are considerably longer. Any gas clouds in the Sun's vicinity 4 Myr ago would have been highly ionized. These two CMa stars left a wake of ionized and heated gas, consistent with the tunnel of low N_{HI} observed in their direction. A high level of ionization was established, peaking at $x \approx 0.99$ during closest stellar passage. The ionization levels of H and He decreased on Myr timescales, tracking the motions of the stars, with non-equilibrium effects setting in during the last 1.6 Myr. In the future, the Sun will exit the local cloud and once again be exposed to a much higher ionizing radiation field unshielded by the local cloud.

4. SUMMARY OF RESULTS AND FUTURE STUDIES

We derived a consistent set of stellar parameters for β CMa (mass, radius, effective temperature, luminosity) consistent with its shorter parallax distance (151 pc vs. 203 pc), interferometric angular diameter ($\theta_d = 0.52 \pm 0.03 \text{ mas}$), and integrated bolometric flux, $f = (36.2 \pm 4.9) \times 10^{-6} \text{ erg cm}^{-2} \text{ s}^{-1}$. From these, we derived $T_{\text{eff}} = 25,180 \pm 1120 \text{ K}$ and $L \approx 10^{4.41 \pm 0.06} L_{\odot}$ and updated values of absolute magnitude ($M_V = -3.93 \pm 0.04$ and $M_{\text{bol}} = -5.97$). On the H-R diagram, the new parameters place β CMa within the β -Cephei pulsational instability strip, consistent with its observed pulsations and the boundaries of theoretical instability on evolutionary tracks (L. Deng & D. R. Xiong 2001). The following points summarize our primary results:

1. The stellar parallax distance and angular diameter of β CMa yield a radius $R = 8.44 \pm 0.56 R_{\odot}$. Bolometric relations between the integrated stellar flux and radius yield an effective temperature $T_{\text{eff}} \approx 25,180 \pm 1120 \text{ K}$ and luminosity $L \approx 10^{4.41 \pm 0.06} L_{\odot}$. Both gravitational and evolutionary masses are consistent at $M \approx 13 \pm 1 M_{\odot}$.
2. From models of the stellar and interstellar attenuation of the ionizing flux in the Lyman continuum, we determine a column density $N_{\text{HI}} = (1.9 \pm 0.1) \times 10^{18} \text{ cm}^{-2}$ in the local cloud, corresponding to optical depth $\tau_{\text{LL}} = 12.0 \pm 0.6$ at the Lyman limit.
3. Using non-LTE model atmospheres and observed EUV spectra, we estimate a stellar flux decrement $\Delta_{\text{star}} = 67 \pm 7$ at the Lyman limit. At the external surface of the local cloud, β CMa produces ionizing photon fluxes of $\Phi_{\text{HI}} \approx 3700 \pm 1000 \text{ cm}^{-2} \text{ s}^{-1}$ and $\Phi_{\text{HeI}} \approx 110 \pm 30 \text{ cm}^{-2} \text{ s}^{-1}$. At a distance $d = 151 \pm 5 \text{ pc}$, its LyC photon production rate is $Q_{\text{H}} \approx 10^{46.0 \pm 0.1} \text{ photons s}^{-1}$.
4. Because of attenuation, the EUV flux from β CMa incident on the local clouds is ~ 20 times higher than viewed from Earth. The photoionization rates at the cloud surface are $\Gamma_{\text{HI}} \approx 1.5 \times 10^{-14} \text{ s}^{-1}$ and $\Gamma_{\text{HeI}} \approx 7.3 \times 10^{-16} \text{ s}^{-1}$. For local gas with $n_{\text{H}} = 0.2 \text{ cm}^{-3}$ and $T \approx 7000 \text{ K}$, photoionized only by ϵ and β CMa, the current ionization fractions at the cloud surface would be $x \approx 0.48$ (H^+) and $y \approx 0.02$ (He^+). They would have been much higher in the past (4.4 Myr ago) when both ϵ CMa and β CMa passed within $10 \pm 1 \text{ pc}$ of the Sun.

Several ionization issues remain, particularly the potentially enhanced level of He^+ ionization. Additional sources of He-ionizing photons could arise from three nearby white dwarfs or from the local hot bubble, a cavity of hot plasma ($T \approx 10^6 \text{ K}$) believed responsible for the soft X-ray background (Snowden et al. 1990; Galeazzi et al. 2014; Yueng et al. 2024). We are exploring such models in a subsequent paper, where we find that the hot bubble could produce ionizing photon fluxes $\Phi_{\text{H}} = 7000\text{--}9000 \text{ cm}^{-2} \text{ s}^{-1}$, comparable to or greater than those of the B stars. Importantly, this emission includes flux in the He I continuum (100–500 Å) produced by a range of ionization states of iron (Fe^{+8} to Fe^{+12}). Recent reviews of the local ISM (J. Slavin & P. Frisch 2008; P. Frisch et al. 2011) suggest mean ionization fractions $x = 0.2\text{--}0.3$ and $y = 0.4\text{--}0.5$, and electron fractions $f_e = 0.24\text{--}0.35$. The elevated He^+ fractions would require $\Gamma_{\text{HeI}} \approx (2\text{--}3)\Gamma_{\text{HI}}$ in photoionization equilibrium conditions. As suggested by Slavin & Frisch (2002), the EUV emission from various Fe ions in the hot plasma may help to explain the elevated He^+/H^+ ionization ratios. Alternatively, the He^+ and H^+ could be out of photoionization equilibrium, as a result of the trajectories of ϵ CMa and β CMa relative to the Sun over the past 4.4 Myr.

Table 1. Various Stellar (β CMa) Parameters^a

Reference Paper	d	T_{eff}	$\log g$	R/R_{\odot}	M/M_{\odot}	L/L_{\odot}	M_{bol}
	(pc)	(K)	(cgs)				(mag)
Cassinelli et al. (1996)	206	$20,990 \pm 760$	3.4 ± 0.15	$16.2^{+1.2}_{-1.2}$	$15.2^{+6.4}_{-4.4}$	$45,900 \pm 9500$	-6.91
Fossati et al. (2015) ^b	151 ± 5	$24,700 \pm 300$	3.78 ± 0.08	$7.4^{+0.8}_{-0.9}$	$12.0^{+0.3}_{-0.7}$	$25,700^{+3800}_{-3800}$	-6.29
Fossati et al. (2015) ^c	151 ± 5	$24,700 \pm 300$	3.78 ± 0.08	$8.2^{+0.6}_{-0.5}$	$12.6^{+0.4}_{-0.5}$	$25,700^{+3800}_{-3300}$	-6.29
Current Study (2025)	151 ± 5	$25,180 \pm 1120$	3.70 ± 0.08	8.44 ± 0.57	13 ± 1	$25,800 \pm 3900$	-5.97

^a Values of effective temperature, surface gravity, radius, mass, luminosity, and bolometric absolute magnitude given in past papers. L. Fossati et al. (2015) derived R and M from two sets of evolutionary tracks (footnotes b and c).

^b Stellar mass and radius inferred from evolutionary tracks of C. Georgy et al. (2013).

^c Stellar mass and radius inferred from evolutionary tracks of L. Brott et al. (2011).

ACKNOWLEDGEMENTS

We thank Emily Witt, James Green, and Kevin France for discussions of the far-UV spectra of β CMa with the Colorado DEUCE rocket. We also thank Jeffrey Linsky, Seth Redfield, and Jon Slavin for scientific discussions about the local ISM. A portion of this study was supported by the New Horizons Mission program for astrophysical studies of cosmic optical, ultraviolet, and Ly α backgrounds.

REFERENCES

- Bethe, H. A., & Salpeter, E. E. 1957, *Quantum Mechanics of One- and Two-Electron Atoms* (Berlin: Springer)
- Bohlin, R. C. 1975, *ApJ*, 200, 402
- Bohlin, R. C., Savage, B. D., & Drake, J. F. 1978, *ApJ*, 224, 132
- Brott, L., de Mink, S. E., Cantiello, M., et al. 2011, *A&A*, 530, A115
- Cassinelli, J. P., Cohen, D. H., MacFarlane, J. J., et al. 1995, *ApJ*, 438, 932
- Code, A. D., Davis, J., Bless, R. C., & Hanbury Brown, R. 1976, *ApJ*, 203, 417
- Craig, N., Abbott, M., Finley, D., et al. 1997, *ApJS*, 113, 131
- Deng, L., & Xiong, D. R. 2001, *MNRAS*, 327, 881
- Draine, B. T. 2011, *Physical Processes in the Interstellar and Intergalactic Medium* (Princeton: Princeton Univ. Press)
- Dupuis, J., Vennes, S., Bowyer, S., Pradhan, A. K., & Thejll, P. 1995, *ApJ*, 455, 574
- Fossati, L., Castro, N., Morel, T., et al. 2015, *A&A*, 574, A20
- Frisch, P. C., Redfield, S., & Slavin, J. D. 2011, *ARA&A*, 49, 237
- Frisch, P. C., & York, D. G. 1983, *ApJ*, 271, L59
- Galeazzi, M., Chiao, M., Collier, M. R., et al. 2014, *Nature*, 512, 171
- Georgy, C., Ekström, S., Granada, A., et al. 2013, *A&A*, 553, A24
- Green, J., Jelinsky, P., & Bowyer, S. 1990, *ApJ*, 359, 499
- Gry, C., York, D. G., & Vidal-Madjar, A. 1985, *ApJ*, 296, 593
- Hanbury Brown, R., Davis, J., & Allen, L. R. 1974, *MNRAS*, 167, 121
- Hillier, D. J., & Miller, D. L. 1998, *ApJ*, 496, 407
- Leitherer, C., Ekström, S., Meynet, G., et al. 2014, *ApJS*, 212, 14
- Lesh, J. R. 1968, *ApJS*, 17, 371
- Linsky, J. L., Redfield, S., & Tilipman, D. 2019, *ApJ*, 886, 41
- Martins, F., Schaerer, D., & Hillier, D. J. 2005, *A&A*, 436, 1049
- Najarro, F., Kudritzki, R. P., Cassinelli, J. P., Stahl, O., & Hillier, D. J. 1996, *A&A*, 306, 892
- Negueruela, I., Simón, S., de Burgos, A., Casasbuenas, A., & Beck, P. G. 2024, *A&A*, 690, A176
- Osterbrock, D. E., & Ferland, G. 2006, *Astrophysics of Gaseous Nebulae and Active Galactic Nuclei* (Sausalito: University Science Books)
- Pauldrach, A. W. A., Hoffmann, T. L., & Lennon, M. 2001, *A&A*, 275, 161
- Pedersen, M. G., Escorza, A., Pápics, P., & Aerts, C. 2020, *MNRAS*, 495, 2738
- Samson, J. A. R., He, Z. H., Yin, L., & Haddad, G. N. 1994, *J Phys B*, 27, 887
- Savage, B. D., Bohlin, R. C., Drake, J. F., & Budich, W. 1977, *ApJ*, 216, 291
- Sfeir, D. M., Lallement, R., Crifo, F., & Welsh, B. Y. 1999, *A&A*, 346, 785
- Shull, J. M., Curran, R. M., & Topping, M. W. 2025, *ApJ*, 971, 21
- Shull, J. M., & Van Steenberg, M. E. 1985, *ApJ*, 294, 599
- Slavin, J. D., & Frisch, P. C. 2002, *ApJ*, 565, 364
- Slavin, J. D., & Frisch, P. C. 2008, *A&A*, 491, 53
- Snowden, S. L., Cox, D. P., McCammon, D., & Sanders, W. T. 1990, *ApJ*, 354, 211
- Vallerga, J. V. 1998, *ApJ*, 497, 921
- Vallerga, J. V., & Welsh, B. Y. 1995, *ApJ*, 444, 702
- van Leeuwen, F. 2007, *A&A*, 474, 653
- Welsh, B. Y. 1991, *ApJ*, 373, 556
- Yeung, M. C. H., Ponti, G., Freyberg, M. J., et al. 2024, *A&A*, 690, A399

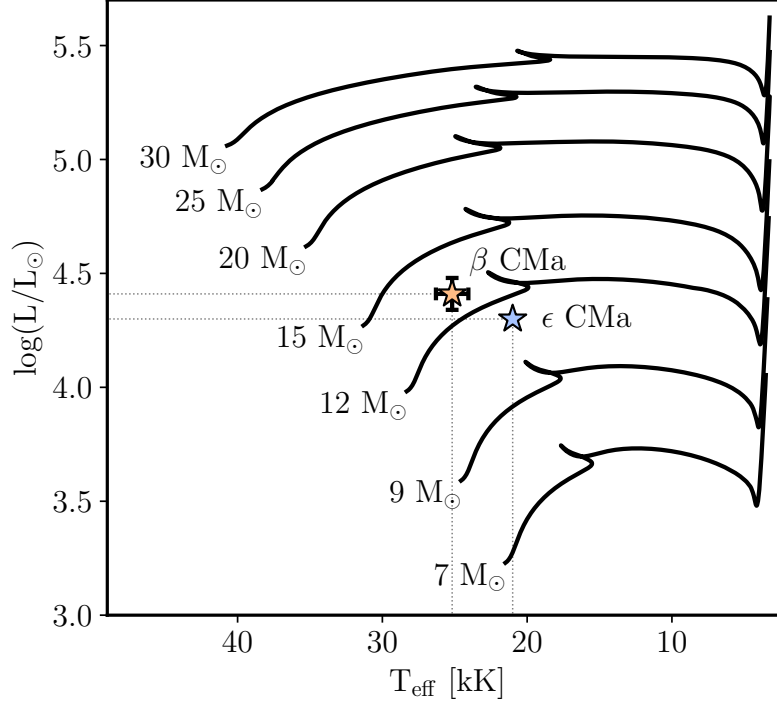


Figure 1. The location of β CMA on the Hertzsprung-Russell diagram is shown for our derived parameters, $\log(L/L_\odot) = 4.41 \pm 0.06$ and $T_{\text{eff}} = 25,180 \pm 1120$ K, based on new radius $R = 8.44 \pm 0.56 R_\odot$ and parallax distance $d = 151 \pm 5$ pc. The evolutionary tracks are from L. Brott et al. (2011) with Milky Way metallicities and initial masses labeled from 7–30 M_\odot . The location of ϵ CMA (J. M. Shull et al. 2025) is shown for comparison.

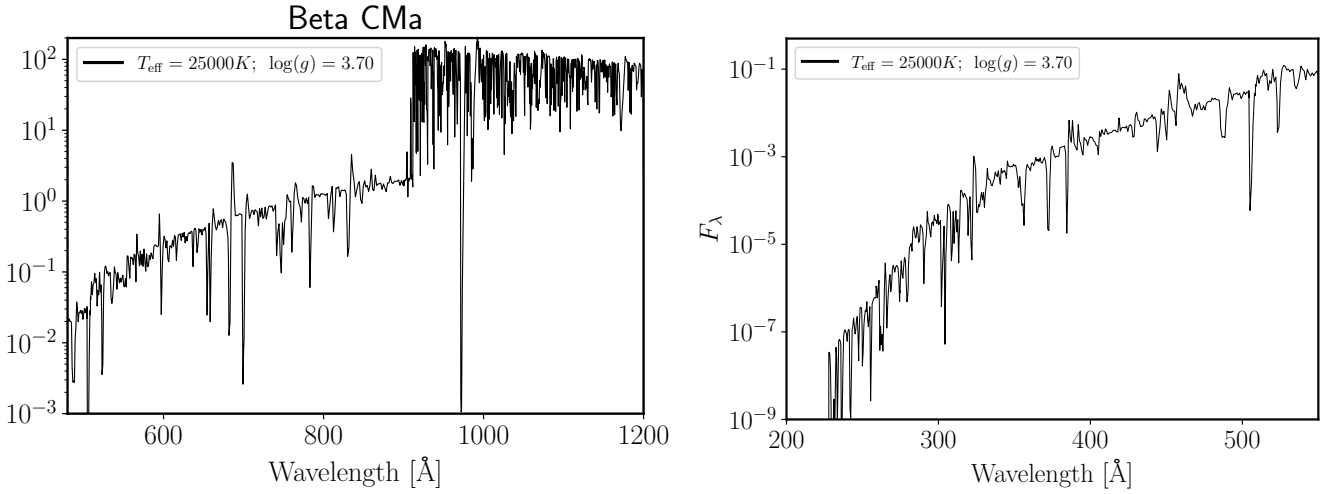


Figure 2. Far-UV and EUV spectra for β CMA from a model atmosphere computed with the non-LTE line-blanketed code **WM-basic** for effective temperature $T_{\text{eff}} = 25,000$ K and surface gravity $\log g = 3.70$. (Left) Flux distribution $\log F_\lambda$ from 850–1200 Å, showing the Lyman limit decrement at 912 Å. (Right) Flux distribution from 228 Å to 550 Å. The absence of an edge at the He I ionization limit (504 Å) is a result of non-LTE effects from backwarming of the upper atmosphere from a solar wind in early B-type stars.